Oligoacetic Acid Characterization by Isocratic and Linear Salt Gradient Anion-Exchange Chromatography

Hong Li[1,2] and **Costas S. Patrickios**[1,3,*]

[1]Department of Chemical Engineering, University of Manchester Institute of Science and Technology (UMIST), P.O. Box 88, Manchester M60 1QD, U.K.; [2]Department of Chemistry, University of Manchester, Oxford Road, Manchester M13 9PL, U.K.; and [3]Department of Chemistry, Faculty of Pure and Applied Sciences, University of Cyprus, P.O. Box 20537, 1678 Nicosia, Cyprus

Abstract

A homologous series of four oligomers of acetic acid (namely acetic acid, succinic acid, tricarballylic acid, and tetracarboxylic acid) is characterized using isocratic and linear salt gradient anion-exchange chromatography. The double logarithmic plot of the isocratic retention factors versus the salt concentration gives straight lines for all samples. These straight lines (with the exception of the line for the strongly retained succinate peak) have a common intersection point—something which is proved to be a direct consequence of the stoichiometric mass-action ion-exchange model. The characteristic charge and the equilibrium ion-exchange constant (and the corresponding Gibbs free energy of ion exchange, or $\Delta G^{exchange}$) are determined from the isocratic experiments. The characteristic charge agrees satisfactorily with the number of carboxylic acid groups in the samples, and the $\Delta G^{exchange}$ value decreases linearly with the characteristic charge. Succinic acid always gives two chromatographic peaks despite the proven chemical purity of the sample. The characteristic charge that is calculated for both of the succinic acid peaks is approximately two. The $\Delta G^{exchange}$ value calculated for the weakly retained succinic acid peak falls in the free energy versus characteristic charge straight line defined by the other homologues. The $\Delta G^{exchange}$ value of the strongly retained peak is lower than that of the weakly retained peak by 1.85 kJ/mol. The two succinic acid peaks are explained in terms of an equilibrium between two conformers in solution—one binding the solution counterions tightly and the other loosely. An analysis of all samples under a linear salt gradient provides retention times that increase linearly with the number of functional groups. Using an appropriate model (along with the isocratically determined characteristic charge and ion-exchange constant), we predict theoretically the linear gradient retention times, which agree reasonably well with the experimental ones.

*Author to whom correspondence should be addressed.

Introduction

Ion-exchange displacement chromatography is a powerful separation technique possessing several advantages over the conventional isocratic, linear gradient, or step gradient techniques, including higher column throughputs and concentrated products (1–3). The distinguishing feature of the process is the use of the displacer, an ionic compound whose affinity for the stationary phase must be higher than that of all of the components of the mixture to be separated. Polyelectrolytes have the required high affinity, but at an excessive degree, rendering difficult their postdisplacement removal for column regeneration. The solution to this problem is the use of oligoelectrolytes (4), which (having just high enough affinity) can be removed from the column much more easily than the corresponding higher molecular weight species.

A detailed characterization of the ion-exchange affinity of such oligoelectrolytes is necessary in order to elucidate the critical structural features governing the adsorption of these molecules. To this end, Cramer and coworkers (5,6) have studied low-molecular-weight amine-based cation-exchange displacers and found that linear compounds have a higher binding affinity than branched or cyclic ones and the presence of aromatic moieties in the displacers increases the binding affinity for most stationary phases. In a similar way, we have characterized three families of carboxylic acid containing potential anion-exchange displacers. The first family was comprised of seven α,ω-alkyl dicarboxylic acids (7) whose ion-exchange affinity was found to be independent of the length of the oligomethylene spacer. Nine benzene oligocarboxylic acids (8) were the members of the second family we characterized. These compounds displayed a binding affinity that was not only dependent on the number of carboxylic acid groups but also dependent on their relative position in the benzene ring. The third family was comprised of a series of six near-monodis-

persed poly(methacrylic acid)s (9), whose retention times in a linear salt gradient were independent of their molecular weights. The present study deals with the characterization of the ion-exchange affinity of a fourth family of carboxylic acids and particularly of the first four lower oligomers of acetic acid, whose chemical formulas and names are presented in Figure 1.

Experimental

Sodium acetate, succinic acid, tricarballylic acid, tetracarboxylic acid, tris(hydroxymethylene) aminomethane (Tris), tris(hydroxymethylene) aminomethane hydrochloride (Tris HCl), sodium chloride, and a 0.5M sodium hydroxide solution were all purchased from Aldrich, U.K. An analytical Protein-Pak Q 8HR Waters (Hertfordshire, U.K.) strong anion-exchange column (100 × 5 mm) packed with 8-µm quaternary methylamine-derivatized beads (100-nm average pore size) was used for the experiments. A Polymer Laboratories (Shropshire, U.K.) LC1150 Quaternary Pump was used to deliver the solvent at a flow rate of 0.5 mL/min. Also, a Polymer Laboratories LC1200 UV–vis detector was used to monitor the column effluent. Sample volumes of 20 µL were introduced using a 7125 Rheodyne (Rohnert Park, CA) injector, and the absorbance was monitored at 230 nm. Experiments were performed at pH 8.0 (Tris buffer containing 28mM Tris HCl) at various salt concentrations (0.0–0.4M NaCl, isocratic experiments), which were achieved by online mixing two pH 8 stock solutions—one with 1.0M NaCl and the other salt-free. In the gradient experiments, the same solutions were used to produce a 10-min linear salt gradient from 0.1 to 1.0M NaCl.

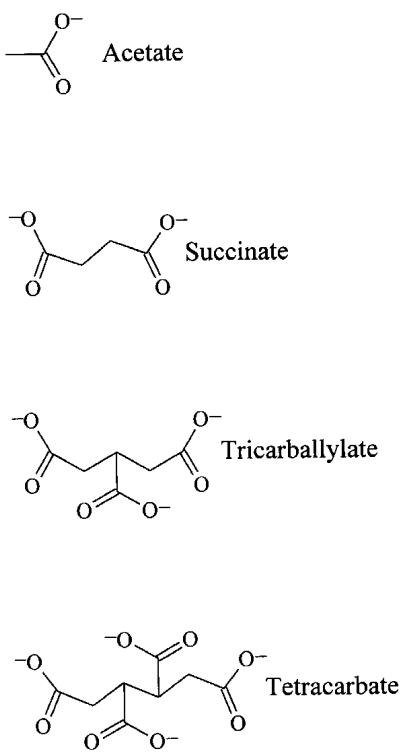

Figure 1. Chemical formulas and names of the four acetic acid oligomers in the fully ionized state.

Results and Discussion

All experiments of this study were performed at pH 8, in which all the carboxylic acid groups in all of the samples were fully dissociated (as shown in Figure 1). This was confirmed by hydrogen ion titration experiments in which it was observed that the full ionization of all samples was achieved from pH 7.

The retention times (t_R) of the samples that were determined under isocratic elution conditions were converted to retention (capacity) factors (k') using the formula (10):

$$k' = (t_R - t_0) / t_0' \qquad \text{Eq. 1}$$

where t_0 is the dead time of the column (which is the elution time of an unretained solute) and t_0' is the column dead time corrected for a noncolumn volume. The k' values and the corresponding salt concentrations were combined to calculate the characteristic charge (ν) and the equilibrium ion-exchange constant (K) from the following equation (11,12):

$$\log k' = \log(K\beta^{\nu}\Lambda^{\nu}) - \nu \log C_{salt} \qquad \text{Eq. 2}$$

where C_{salt} is the total solution concentration of counterions to the stationary phase (chloride in this case), β is the column phase ratio, and Λ the column capacity in monovalent anions. The values of β and Λ were taken to be 0.5518 mL stationary phase per milliliter of mobile phase and 487mM monovalent ions, respectively, in agreement with previous reports (8,13).

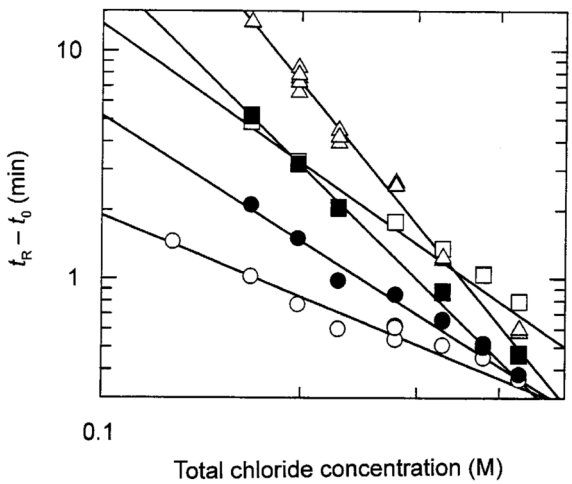

Figure 2. Double-logarithmic plots of the oligoacetate retention times as a function of the salt concentration in the mobile phase: acetate, ○; weakly retained succinate, ●; strongly retained succinate, □; tricarballylate, ■; and tetracarbate, △.

The ion-exchange Gibbs free energy ($\varnothing G^{exchange}$) was calculated from K using the following equation (11):

$$\Delta G^{exchange} = -RT \ln K \qquad \text{Eq. 3}$$

where R is the gas constant and T the absolute temperature.

Figure 2 is the double-logarithmic plot of $t_R - t_0$ against C_{salt}, the latter of which also includes the chloride anions coming from Tris HCl. All of the series of data fell on straight lines, from which ν and $\varnothing G^{exchange}$ were calculated using equations 2 and 3.

Figure 3 plots the ν values of the samples against the number of carboxylic acid groups. There were two points for succinic acid (with approximately the same characteristic charge) because of the double chromatographic peak of this sample, which will be discussed. The values for the characteristic charge of the oligoacetates were close to and always lower than the number of carboxylic acid groups. This discrepancy increased with the homologue size. This can be seen clearly in the figure by observing the position of the points relative to the straight line of unit slope passing from the origin. This implies that all of the carboxylic acid groups of all samples were most of the time in contact with the oppositely charged groups of the ion-exchange surface, which was a consequence of the small size of our analytes. However, the register with the surface became slightly but systematically more difficult as the sample size increased. A deviation of the characteristic charge from the number of ionic groups has also been observed with oligonucleotides (14). This has been attributed to the three-dimensional structure of the samples, although linear oligomers (the placement of the ionic groups on side chains of the carbon backbone in combination with the carbon tetrahedral angle) lead to a helical arrangement of the functional groups. Another possible cause is the chain configurational entropy loss upon the adsorption of all functional units. This entropy loss would be much greater for the larger samples, which would simply lead to the adsorption of a smaller percentage of ionic groups. In contrast, the characteristic charge of the benzene oligocarboxylic acids always agreed well (up to the maximum charge of 6) with the number of carboxylic acid groups (8). This could be because of the shape of these samples, in which the flat benzene scaffold would most likely ensure the possibility that all of the carboxylic acid groups would lie in the same plane.

Figure 4 shows the dependence of $\varnothing G^{exchange}$ on the number of functional groups in the oligoacetates. There were two points for succinate (at the point corresponding to two carboxylates) because this sample presented two peaks. The $\varnothing G^{exchange}$ value decreased linearly (considering only the weakly retained succinate peak) with the number of carboxylic acid groups, indicating a more favorable interaction of the higher homologues with the surface. The linearity in the trend was consistent with the well-documented observations of Martin (15) for the hydrocarbon retention on silica or reverse-phase columns. It also implied a constant increment in the energy of exchange for the addition of an extra monomer unit in the homologous series. The average value of this increment was calculated from our data to be –1.24 kJ/mol, which was in good agreement with the value of –1.46 kJ/mol calculated as the increment per carboxylic acid group in benzene oligocarboxylic acids (8). This was also in fair agreement with the monomer repeat unit increment in poly(methacrylic acid)s of approximately –1.8 kJ/mol (9).

Equation 4 gives the linear fit to the data (plotted as a dashed line in Figure 4):

$$\varnothing G^{exchange} = 5.02 - 1.24n \qquad \text{Eq. 4}$$

where n represents the number of carboxylic acid groups.

Figure 5 plots the $\varnothing G^{exchange}$ value of the oligoacetates against their characteristic charge. This figure is very similar to Figure 4 in that again there was a linear dependence between the two variables, but the slope was slightly greater than the slope in Figure 4 because the characteristic charge was slightly smaller than the number of carboxylic acid groups (see Figure 3). The dashed line connecting the data points in Figure 5 is given by the equation:

$$\varnothing G^{exchange} = 5.36 - 1.59\nu \qquad \text{Eq. 5}$$

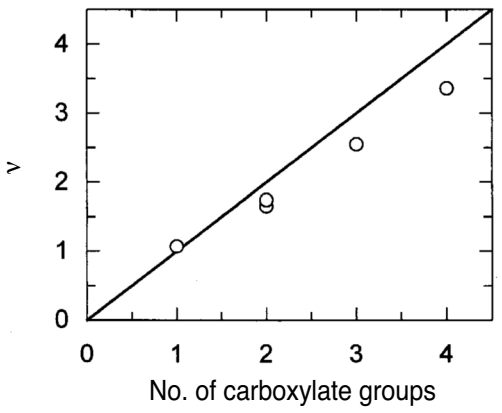

Figure 3. Dependence of ν on the number of functional groups in the oligoacetates.

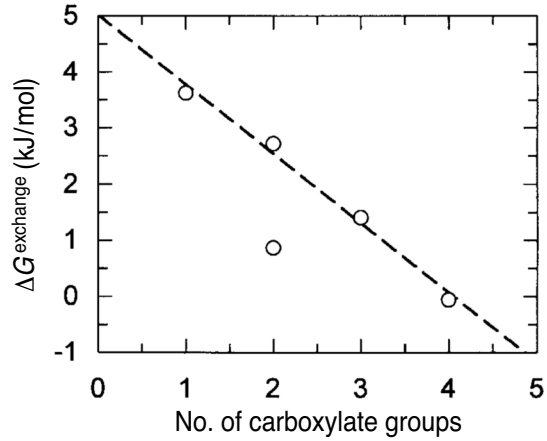

Figure 4. Dependence of $\Delta G^{exchange}$ on the number of functional groups in the oligoacetates.

whose slope is greater (in absolute value) than that of equation 4 for the reason explained previously. It should be noted that the slope of equation 5 is in better agreement with the literature values of –1.5 kJ/mol (8) and –1.8 kJ/mol (9) than the slope of equation 4.

The presence of two succinate peaks with the same characteristic charge of two and a difference in their $\Delta G^{exchange}$ values of approximately 2 kJ/mol has been observed previously (7). This has been attributed to an equilibrium between two main succinic acid conformers in solution: one form of succinic acid that tightly binds sodium counterions in solution that can be only weakly adsorbed and the other that loosely binds counterions that can be strongly adsorbed (7). Our sample of succinic acid was chemically pure, as confirmed by proton nuclear magnetic resonance spectroscopy and gel-permeation chromatography in tetrahydrofuran. Moreover, the explanation that the second peak was a result of anhydride formation is precluded, because this would lead to an unretained peak with a zero characteristic charge (anhydrides are nonionic). It should be noted that other α,ω–dicarboxylic acid homologues of succinic acid have given only one chromatographic peak (7).

All straight lines (with the exception of that for the strongly retained succinate peak) in Figure 2 presented a common point of intersection located at a value for C_{salt} of 0.525M. We decided to explain this interesting observation using the stoichiometric mass-action ion-exchange theory. First, we wrote the $\Delta G^{exchange}$ value of a ν-mer in the form of equations 4 and 5:

$$\Delta G^{exchange} = \Delta G_0 + \nu \Delta g \qquad \text{Eq. 6}$$

where ΔG_0 is a constant equal to the $\Delta G^{exchange}$ of the uncharged monomer (undissociated acetic acid in this study) and Δg is the constant increment of $\Delta G^{exchange}$ per additional monomer repeat unit.

Using equation 3, equation 6 can be transformed to:

$$K = K_0 \kappa^{\nu} \qquad \text{Eq. 7}$$

where K_0 is the equilibrium ion-exchange constant of the uncharged monomer given by:

$$\Delta G_0 = -RT \ln K_0 \qquad \text{Eq. 8}$$

and κ is the equilibrium ion-exchange constant per added monomer repeat unit defined by:

$$\Delta g = -RT \ln \kappa \qquad \text{Eq. 9}$$

Rewriting equation 2 in the exponential (as opposed to the logarithmic) form, we have:

$$k' = K (\beta\Lambda / C_{salt})^{\nu} \qquad \text{Eq. 10}$$

Combining equation 10 with equation 7, we get for k':

$$k' = K_0 (\kappa\beta\Lambda / C_{salt})^{\nu} \qquad \text{Eq. 11}$$

Writing equation 11 for the monomer (ν = 1), we get for the monomer retention factor (k_1'):

$$k_1' = K_0 (\kappa\beta\Lambda / C_{salt}) \qquad \text{Eq. 12}$$

The intersection of all the log k' versus logC_{salt} lines was equivalent to the intersection of the monomer line with each one of the lines of all the higher oligomers at the same point. This implied the equality of log k_1' to the log k' values of all the higher oligomers at some logC_{salt} value. Thus, at the intersection point we have k' being equal to k_1', which with the use of equations 11 and 12 results in:

$$(\kappa\beta\Lambda / C_{salt})^{\nu} - (\kappa\beta\Lambda / C_{salt}) = 0 \qquad \text{Eq. 13}$$

or

$$(\kappa\beta\Lambda / C_{salt})^{\nu-1} = 1 \qquad \text{Eq. 14}$$

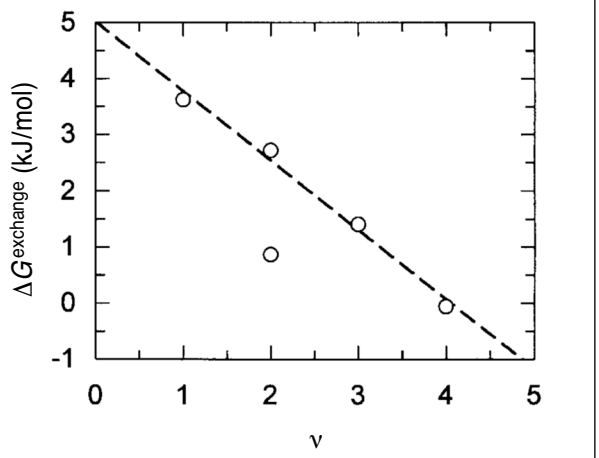

Figure 5. Dependence of $\Delta G^{exchange}$ on the ν value of the oligoacetates.

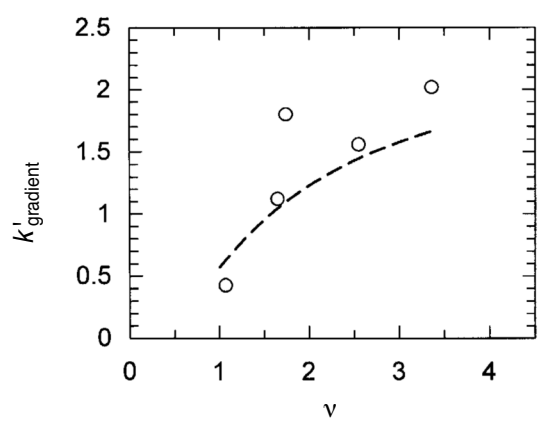

Figure 6. Dependence of $k'_{gradient}$ on the ν value of the oligoacetates. The dashed curve represents the prediction of the theory.

which simply means that at the intersection point, the following equation is valid:

$$(\kappa\beta\Lambda / C_{salt}) = 1 \qquad \text{Eq. 15}$$

Because equation 14 applies for all values of ν greater than 1, the intersection of the monomer log k' versus the logC_{salt} line with those for all of the higher homologues will take place at the same point, which is the theoretical confirmation of our experimental observation. Using equation 15 along with the known values of β and Λ and the value of C_{salt} at the intersection point of 0.525M, we can get an estimate for κ. This gives us the value κ = 1.95, which using equation 9 provides Δg = –1.63 kJ/mol.

This is in excellent agreement with the slope of equation 5 (–1.59 kJ/mol), which was calculated from the data of Figure 5. Thus, the salt concentration at the common intersection point of the log k' versus logC_{salt} lines of the homologous family of oligomers provided an alternative and convenient method for the calculation of the $\Delta G^{exchange}$ increment per characteristic charge.

Figure 6 shows the k' values measured under a linear salt gradient (0.1 to 1.0M NaCl) as a function of the characteristic charge of the oligoacetates. An almost linear relationship was observed between the two variables. The dashed line in the figure lying close to the experimental points represented the prediction of a theoretical equation (8,16) based on the stoichiometric mass-action ion-exchange model:

$$k' = \frac{t_d}{t_0} + \frac{1}{G}\left\{\left[(\nu+1)G\left(K\beta^{\nu}\Lambda^{\nu} - \frac{t_d}{t_0}C_0^{\nu}\right) + C_0^{\nu+1}\right]^{\frac{1}{\nu+1}} - C_0\right\} \qquad \text{Eq. 16}$$

where t_d is the delay time of the gradient caused by the volume of the mixing chamber, C_0 is the initial salt concentration in the gradient, and G is the gradient's slope. The G value is calculated by:

$$G = \frac{C_F - C_0}{t_G / t_0} \qquad \text{Eq. 17}$$

where C_F is the final salt concentration in the gradient and t_G is the duration of the salt gradient.

In plotting equation 16, K was obtained from:

$$K = 0.111 \times 1.922^{\nu} \qquad \text{Eq. 18}$$

which was derived by combining equations 5 and 7 using the isocratic results. The reasonable agreement observed in Figure 6 between the gradient data and the theoretical predictions employing isocratic data showed the validity of the theory and the internal consistency of our experimental methods.

Conclusion

We have presented a systematic investigation on the anion-exchange chromatographic behavior of the four lower oligomers of acetic acid: acetic acid, succinic acid, tricarballylic acid, and tetracarboxylic acid. Isocratic elution under various salt concentrations allowed the calculation of the characteristic charge and the $\Delta G^{exchange}$ values for all samples. The value of the characteristic charge closely matched the value of carboxylic acid groups in each sample, implying that all the functional groups of the samples were in contact with oppositely charged groups on the surface. A more careful examination revealed that there was a slight negative deviation of the characteristic charge from the number of functional groups, which increases with the sample size. This can be attributed mainly to the nonflat, three-dimensional structure of the oligomers, which becomes more pronounced for the higher oligomers. The $\Delta G^{exchange}$ value decreased linearly with the characteristic charge, suggesting a constant contribution per carboxylic acid group. The oligomers of this study presented different retention times under a linear salt gradient, which increased approximately linearly with the oligomer size. Under both isocratic and linear salt gradient elution, succinic acid presented two chromatographic peaks. An analysis of the isocratic data revealed a characteristic charge of two for both peaks and a $\Delta G^{exchange}$ value for the high-affinity peak, which was more favorable than that of the weakly retained peak by –1.9 kJ/mol. We attribute this to the existence of two succinic acid conformers in the solution: one with tightly bound sodium counterions with low affinity for the surface and one with no or loosely bound sodium and a high affinity for the surface.

Acknowledgments

We are grateful to the Biotechnology and Biological Sciences Research Council (U.K.) for funding this work (grant no. 36/T0 7395). We would also like to thank Dr. Lars Hagel of Pharmacia Biotech (Sweden) for kindly donating the chromatographic media that were used in the beginning of this study.

References

1. R. Freitag. Displacement chromatography for biopolymer separation. *Nature Biotechnol.* **17:** 300–302 (1999).
2. I.Y. Galaev, P. Arvidsson, and B. Mattiasson. Protein displacement in dye-ligand chromatography using neutral and charged polymers. *J. Molec. Recogn.* **11:** 255–60 (1998).
3. S.M. Cramer. Displacement chromatography. *Nature* **351:** 251–52 (1991).
4. S.-C. David Jen and N.G. Pinto. Use of the sodium salt of poly(vinylsulfonic acid) as a low-molecular-weight displacer for the protein separations by ion-exchange displacement chromatography. *J. Chromatogr.* **519:** 87–98 (1990).
5. A.A. Shukla, K.A. Barnthouse, S.S. Bae, J.A. Moore, and S.M. Cramer. Structural characteristics of low-molecular-mass displacers for cation-exchange chromatography. *J. Chromatogr. A* **814:** 83–95 (1998).

6. A.A. Shukla, S.S. Bae, J.A. Moore, and S.M. Cramer. Structural characteristics of low-molecular-mass displacers for cation-exchange chromatography. II. Role of the stationary phase. *J. Chromatogr. A* **827:** 295–310 (1998).
7. A.R. Khan and C.S. Patrickios. α,ω-Alkyl dicarboxylic acids: characterization by isocratic anion-exchange chromatography. *J. Chromatogr. Sci.* **37:** 150–54 (1999).
8. H. Li, L. Lue, and C.S. Patrickios. Benzene oligocarboxylic acids: characterization by isocratic, linear gradient, and frontal anion-exchange chromatography. *J. Chromatogr. Sci.* **37:** 413–22 (1999).
9. A. Freydank, T. Krasia, G.J.T. Tiddy, and C.S. Patrickios. Near-monodisperse sodium polymethacrylates: characterization by linear salt gradient anion-exchange chromatography. *J. Chromatogr. Sci.* **38:** 185–88 (2000).
10. P.C. Wankat. *Rate Controlled Separations*. Elsevier Science, New York, NY, 1990.
11. C.S. Patrickios and E.S. Patrickios. Stoichiometric mass-action ion-exchange model: explicit isotherms for monomeric, dimeric, trimeric and tetrameric ions. *J. Chromatogr. A* **694:** 480–85 (1995).
12. C.S. Patrickios and E.N. Yamasaki. A correction to the calculation of the Gibbs free energy of adsorption for biomolecules in ion-exchange systems. *Biophys. Chem.* **69:** 219–20 (1997).
13. C.S. Patrickios, S.D. Gadam, W.R. Hertler, S.M. Cramer, and T.A. Hatton. Block methacrylic polyampholytes as protein displacers in ion-exchange chromatography. *Biotechnol. Prog.* **11:** 33–38 (1995).
14. R.R. Drager and F.E. Regnier. Application of the stoichiometric displacement model of retention to anion-exchange chromatography of nucleic acids. *J. Chromatogr.* **357:** 147–55 (1986).
15. G. Glöckner. Analysis of compositional and structural heterogeneities of polymers by non-exclusion HPLC. *Adv. Polymer Sci.* **79**: 159–214 (1986).
16. S.R. Gallant, S. Vunnum, and S.M. Cramer. Optimization of preparative ion-exchange chromatography of proteins: linear gradient separations. *J. Chromatogr. A* **725:** 295–314 (1996).

Manuscript accepted December 12, 2000.